Operational Atmospheric Correction of Landsat TM Imagery

O. Arino[1], E. Vermote[2] & V. Spaventa[3]

[1]Earth Observation Division, ESRIN, Frascati
[2]NASA-GSFC, Greenbelt, Maryland, USA
[3]SACS, via Paolo Frisi 71A, 00197 Rome, Italy

Thematic Mapper Products derived from Landsat data are corrected operationally for atmospheric effects using meteorological data from ECMWF. The software is based on the radiative transfer code 6S which has been parameterised to retrieve surface reflectance in the 6 TM visible and NIR channels from the top-of-atmosphere radiance. The products are now available from Kiruna and Fucino stations with the nominal mini-, quarter- or full-scene sizes as standard system-corrected products. The 'Rush service' will be provided with a minimum time delay from data take of 36 hours.

Introduction

As a follow-on to the Landsat Thematic Mapper (TM) product line, ESA can now provide a new data product which consists of surface reflectance information contained in the six visible and near infrared channels, corrected for atmospheric effects. This product is suitable for direct parameterisation of land surface processes, for multitemporal surface characterisation and for time series and change analysis. In addition to the scientific value of this product, the user will get improved radiometric contrast and an easier way of producing mosaics made up of images taken at different times.

The removal of perturbations of the satellite signal due to Rayleigh and aerosol scattering and gaseous absorption in the atmosphere is a problem. The solution is to use a model of the state of the atmosphere at sensing time. The surface reflectance is parameterised as a function of the gaseous transmissions, the Rayleigh and aerosol transmission, the spherical albedo, the atmospheric reflectance and the reflectance of the top of the atmosphere (ToA). The latter can be measured by the satellite (*Tanre et al. 1981*) :

- gaseous transmissions are computed knowing the gaseous components of the atmosphere which have a high spatial and temporal dependency; these transmissions vary with species as well as with wavelength;
- molecular (Rayleigh) scattering is dependent of surface pressure and wavelengths;
- aerosol scattering has a variable spectral dependency and a high spatial and temporal dependency.

The System

The atmospheric correction system comprises two separate components: one produces archives of atmospheric data and the other corrects for atmospheric effects.

The ESRIN atmospheric data archiver stores ECMWF data received by the Internet standard file transfer protocol. Thereafter it extracts surface temperature and pressure, processes data giving the integrated water vapour content, and then performs consistency check (display, compare and test). Finally it computes the station coverage of supplementary data such as surface temperature and pressure and total-column water vapour content.

The ECMWF/TOGA basic level 3-A consolidated dataset *(ECMWF 1993)* has been selected because it is appropriate for the required corrections. The data types used are the global surface and upper air (15 pressure levels) data at 00:00 UTC and 12:00 UTC with a resolution of 2.5° in both regular latitude and longitude. Based on estimation of historic data reprocessing requirements, data from 1992 onwards were acquired. Ozone value are derived from maps prepared by *London et al. 1976*. It is possible that data collected by the ozone monitoring instruments GOME and TOMS will be used in the future.

When ECMWF data are corrupted or lack climatological information, default values are taken by the software in the following order of ranking:

- surface pressure computed from ETOPO-5 data, the default value is 1023 mb;
- statistics of water vapour contents published by *Oort 1983*, the default value is 2.4 g/cm^2;
- surface temperature, the default value at 293 K.

The ESRIN atmospheric correction component (bands 1-5 and 7) takes as inputs the extracted meteorological and climatological default value of centre scene (full, quarter, mini), the calibration coefficient *(Thorne et al. 1993)* and the TM data files (1-5 and 7). It provides as output the corrected reflectance scaled by a factor of 400 supplemented by quality control information *(ESA Earthnet 1997)*.

For 16 grid points in the image (6 bands), the processor computes the aerosol optical thickness (AOT) and its standard deviation which are both

band-dependent. It also derives information on the solar and viewing zenith angles and relative azimuth angle, the water vapour and ozone content, surface pressure and surface temperature (value and cloud statistics).

The Algorithm

The algorithm can be decomposed in several steps:

- calibration *(Thorne et al. 1993)*
- cloud masking procedure *(Stowe et al. 1991)*
- AOT inversion
- interpolation between the AOT grid
- computation of grid correction parameters
- pixel reflectance computation *(Vermote et al. 1997)*
- adjacency effects *(Putsay 1992)*.

The correction parameters are computed at every grid point (there are 16 grid points within the image whatever the scene size). The surface reflectance is then extracted by applying bi-linear interpolation to derive the correction parameter for every image pixel.

The cloud masking is derived from reflectance information contained in channels 3 and 4 and temperature information in channel 6, following the method of *Stowe et al. 1991*. A cloud shadow mask is generated by taking into account the viewing geometry as well as the cloud-top height evaluated from brightness temperature in channel 6. Cloudy, shadow and mixed pixels are discarded from further processing.

The retrieval of AOT uses the dark dense vegetation (DDV) technique which allows a dark surface to be identified, using data from channel 7. The AOT in the 3 first channels is then inverted by means of a pre-computed LUT of the scattering transmissions, the spherical albedo and the atmospheric reflectance to provide ten AOTs as a function of observation angle. When no DDV is found in one of the 16 grid cells, missing data are supplied by bilinear interpolation between other grid points. When no DDV surface is found at all, an AOT of zero is assumed.

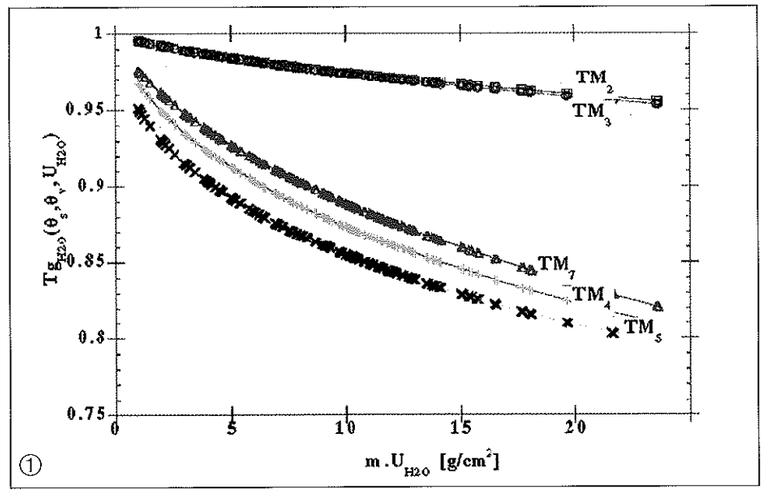

Comparison of approximate and exact transmission (6S) computations of water vapour for each TM channel under various conditions.

With the correction parameter computed at each grid point, the surface reflectance is computed for every non-discarded pixel (cloud, mixed, shadow). A ceiling factor of 400 is applied to the surface reflectance to better fit within one byte.

The correction of the adjacency effects has been implemented based on the work of *Tanre et al. 1981* and that of *Putsay 1992*. The validation phase showed that the time consumed by this process was out of proportion to the gain in quality and this approach was abandoned due to limitations in computer resources.

Results

Figure 1 shows the results of the parameterising of the 6S model for the TM channels and different water vapour contents and angular conditions. Note that impact of water vapour (absorption) is greater for the near infrared channels (TM 4, 5 and 7) than for the visible channels (TM 1, 2, 3).

Comparison of the approximate and exact computed transmission (6S) of ozone for each TM channel under various conditions.

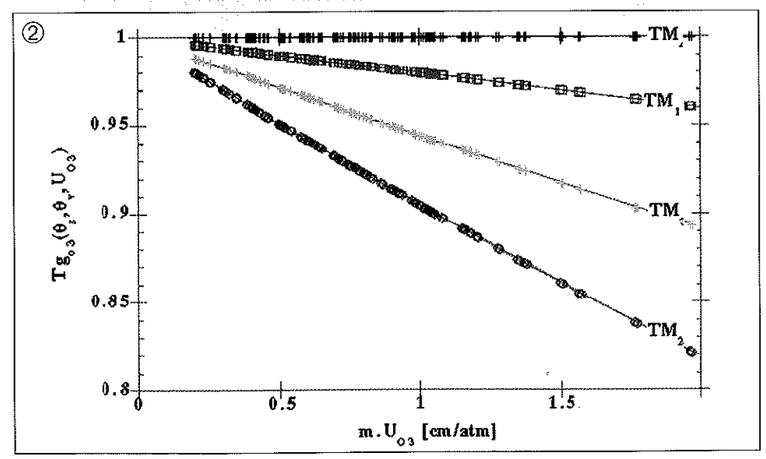

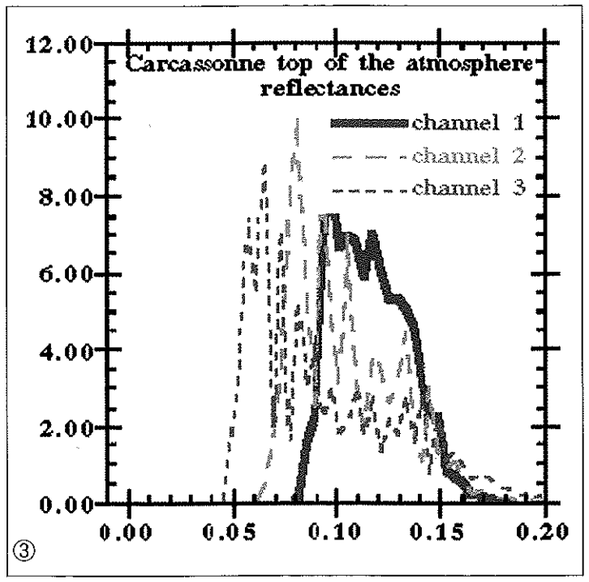

Histograms of data taken from the first three TM channels before atmospheric correction.

Figure 2 shows the results of the 6S parameterisation for ozone transmission as a function of ozone content and observation angle. As expected, the greater impact of ozone absorption is visible for channel 2, while near infrared channels are hardly perturbed.

Figure 3 shows histograms of the three first TM channels taken from a quarter scene of the south-west of France, acquired at Fucino on 1st July 1994. The scene is a mixture of vegetated surfaces (vineyards, agricultural land and forests) and mountainous areas such as the Pyrénées and Corbières. The forms of the histograms of the three natural colour channels appear much as expected.

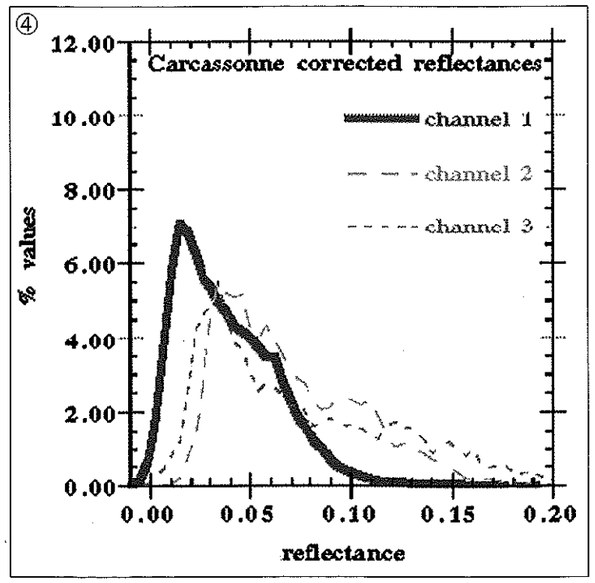

Histograms of the data taken from the first three TM channels after atmospheric correction.

Figure 4 presents histograms of the same three TM channels for the same scene, but with corrected images. A broadening of the three histograms is evident. This is due to dependence of atmospheric correction on the type of surface which tends to increase the contrast between low and high reflective surfaces. Also noticeable is a general reduction in reflectance values. This is normal since the contribution of atmospheric Rayleigh and aerosol scattering in the visible channels is higher than the ozone absorption (Fig. 2) and correcting the atmospheric effect tends to decrease the reflectance values at that wavelength. By contrast, the reflectance values found in channels 4, 5 and 7 increase after correction as a result of the weak component of Rayleigh and aerosol scattering and the high water vapour absorption (Fig. 1).

Figure 5 is the truth colour composite 3/2/1, without atmospheric correction, of the quarter-scene previously used to derive the histograms. A foggy appearance is evident, due to the high concentration of water vapour in the atmosphere during summer which reached 4 g/cm^2 and a visibility of 15 km.

Figure 6 is the same scene but corrected, and the removal of the fogginess and improved contrast can be seen. The same quarter scene was processed at a different period of the year with the benefit that reflectance values were comparable apart from those taken over seasonally vegetated areas (specifically in channel 4).

Conclusion

Landsat TM products can be operationally corrected from the atmospheric effects. One of the best available scientific models has been parameterised to work in an operational environment with affordable processing time. The corrections are dependent on meteorological data collected at sensing time (ECMWF analysis). The validation phase has proved successful. This atmospherically corrected product is now the standard system-corrected TM product.

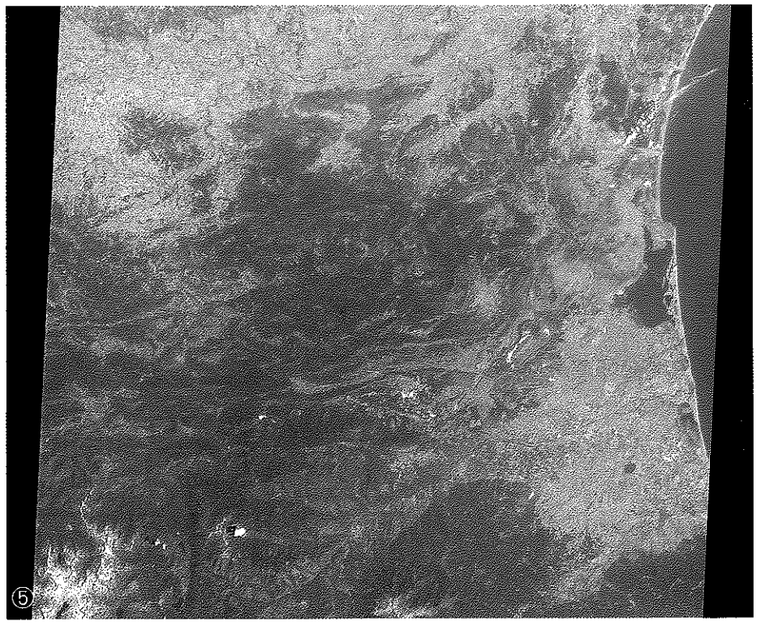

Top-of-the-atmosphere colour composite produced from bands 3, 2 and 1 data of Landsat-5 TM, acquired at Fucino on 1 July 1994.

Surface reflectance colour composite produced from from bands 3, 2 and 1 data of Landsat-5 TM, acquired at Fucino on 1 July 1994.

References

ECMWF, 1993. *The description of the ECMWF/WCRP Level III Global Atmosphetic Data Archive*, ECMWF, Reading, UK.

ESA - Earthnet, 1997. *Landsat TM ESA Product Format Definition*, rev. 2.0, ESA - ESRIN. Frascati, Italy.

London J, DR Bojkov, S Oltmans & JL Kelly, 1976. *Atlas of the Global Distribution of Total Ozone, July 1957-June 1967*, NCAR/TN/113 + STR, NCAR, Boulder, Colorado, USA.

Oort AH, 1983. *Global Atmospheric Circulation Statistics*, 1958-1973, NOAA. Professional Paper 14, Rockville, MD, USA.

Putsay M, 1992. A Simple Atmospheric Correction for the Short-Wave Satellite Image, *Int. Jl. Remote Sensing*, **13**, 1549-1558.

Stowe IL, EP Mc Clain, R Carey, P Pelligrino, GG Gutmann, P Davis, C Long & S Hart, 1991. Global Distribution of Cloud Cover Derived from NOAA/AVHRR Operational Satellite Data, *Adv. Space Res.* **11**, 51-54.

Tanre D, M Herman & PY Deschamps, 1981. Influence of the Background Contribution upon Space Measurements of Ground Reflectance, *Applied Optics*, **20**, 3673-3684.

Thome KJ, DI Gellman, RJ Parada, SF Biggar, PN Slater & NS Moran, 1993. In-flight Radiometric Calibration of Landsat-5 Thematic Mapper from 1984 to Present, *Proc. SPIE*, Orlando, Fl., USA. 12-16 April 1993, pp 1938-1940.

Vermotte EF, D Tanre, JL Deutze, M Herman & J Morcrette, 1997. Second Simulation of the Satellite Signal in the Solar Spectrum, An Overview, *IEEE Trans. Geoscience & Remote Sensing*. **35**, 3 (In press).